The Zel'dovich approximation

Martin White[1,2]

[1] *Departments of Physics and Astronomy, University of California, Berkeley, CA 94720, USA*

[2] *Lawrence Berkeley National Laboratory, 1 Cyclotron Road, Berkeley, CA 94720, USA*

9 December 2014

ABSTRACT

This year marks the 100th anniversary of the birth of Yakov Zel'dovich. Amongst his many legacies is the Zel'dovich approximation for the growth of large-scale structure, which remains one of the most successful and insightful analytic models of structure formation. We use the Zel'dovich approximation to compute the two-point function of the matter and biased tracers, and compare to the results of N-body simulations and other Lagrangian perturbation theories. We show that Lagrangian perturbation theories converge well and that the Zel'dovich approximation provides a good fit to the N-body results except for the quadrupole moment of the halo correlation function. We extend the calculation of halo bias to 3rd order and also consider non-local biasing schemes, none of which remove the discrepancy. We argue that a part of the discrepancy owes to an incorrect prediction of inter-halo velocity correlations. We use the Zel'dovich approximation to compute the ingredients of the Gaussian streaming model and show that this hybrid method provides a good fit to clustering of halos in redshift space down to scales of tens of Mpc.

Key words: gravitation; galaxies: haloes; galaxies: statistics; cosmological parameters; large-scale structure of Universe

1 INTRODUCTION

This year marks the 100th anniversary of the birth of Yakov Zel'dovich, who was a pioneer in the study of large-scale structure and introduced the approximate dynamics that bears his name (Zel'dovich 1970). The Zel'dovich approximation provides an intuitive way to understand the emergence of the beaded filamentary structure which has become known as the cosmic web and a fully realized (though approximate) model of non-linear structure formation (Peebles 1980; Coles & Lucchin 1995; Peacock 1999). The Zel'dovich approximation predicts the rich structure of voids, clusters, sheets and filaments observed in the Universe (Doroshkevich et al. 1980; Pauls & Melott 1995), and indeed it provides a reasonably good match to N-body simulations on large scales (Coles, Melott & Shandarin 1993; Tassev & Zaldarriaga 2012a,c). For a discussion of why the Zel'dovich approximation works so well, see Buchert (1989); Pauls & Melott (1995); Yoshisato et al. (2006); Tassev (2014a). For reviews of the Zel'dovich approximation, see the textbooks referenced above and Shandarin & Zeldovich (1989); Sahni & Coles (1995); Coles & Sahni (1996); Gurbatov, Saichev & Shandarin (2012); Hidding, Shandarin & van de Weygaert (2014).

The last few years have seen a resurgence of interest in the Zel'dovich approximation. It has been applied to understanding the effects of non-linear structure formation on the baryon acoustic oscillation feature in the correlation function (Padmanabhan & White 2009; McCullagh & Szalay 2012; Tassev & Zaldarriaga 2012a) and to understanding how "reconstruction" (Eisenstein, et al. 2007) removes those non-linearities (Padmanabhan, White & Cohn 2009; Noh, White & Padmanabhan 2009; Tassev & Zaldarriaga 2012b).

It has been used as the basis for an effective field theory of large-scale structure (Porto, Senatore & Zaldarriaga 2014). It has been compared to "standard" perturbation theory (Tassev 2014a), extended to higher orders in Lagrangian perturbation theory (Matsubara 2008a,b; Okamura, Taruya, & Matsubara 2011; Carlson, Reid & White 2013) and to higher order statistics (Tassev 2014b). Despite the more than 40 years since it was introduced, the Zel'dovich approximation still provides one of our most accurate models for the distribution of cosmological objects.

In this paper we investigate to what extent the Zel'dovich approximation can be used as a quantitatively accurate model of the low-order clustering of objects in cosmology. The outline is as follows. After some background and review to establish notation in Section 2 we present a derivation of the 2-point function within the Zel'dovich approximation (see also Carlson, Reid & White 2013; Tassev 2014a,b) both for matter (Section 3) and for biased tracers (Section 4). In these sections we show that the principle ingredient to the calculation, the Lagrangian correlator, can be inverted analytically and thus the correlation function expressed as a simple quadrature. All of the ingredients to the Zel'dovich approximation involve only one dimensional integrals of the linear theory power spectrum, and these can be efficiently precomputed and tabulated, making numerical evaluation fast and efficient. We compare the Zel'dovich calculation to some other Lagrangian perturbation theory schemes, and to the results of N-body simulations, in Section 5. We extend previous calculations of the effects of bias to higher order and include non-local, Lagrangian bias in Section 6. Finally we introduce the Zel'dovich Streaming Model (ZSM) as a

hybrid method for accurately computing the redshift-space correlation function of biased tracers in Section 7 and end with a discussion of our results in Section 8.

For plots and numerical comparisons we assume a ΛCDM cosmology with $\Omega_m = 0.274$, $\Omega_\Lambda = 0.726$, $h = 0.7$, $n = 0.95$, and $\sigma_8 = 0.8$. Our simulation data are derived from a suite of 20 N-body simulations run with the TreePM code described in White (2002). Each simulation employed 1500^3 equal mass ($m_p \simeq 7.6 \times 10^{10} \, h^{-1} M_\odot$) particles in a periodic cube of side length $1.5 \, h^{-1}$Gpc as described in (Reid & White 2011; White et al. 2011). Halos are found using the friends-of-friends method, with a linking length of 0.168 times the mean inter-particle spacing.

2 BACKGROUND AND REVIEW

In this section we provide a brief review of cosmological perturbation theory, focusing on the Lagrangian formulation[1] (Buchert 1989; Moutarde et al. 1991; Hivon et al. 1995; Taylor & Hamilton 1996). This material should be sufficient to remind the reader of some essential terminology, and to establish our notational conventions. Our notation and formalism follows closely that in Matsubara (2008a,b); Carlson, Reid & White (2013); Wang, Reid & White (2013) to which we refer the reader for further details.

In terms of the fractional density perturbation, δ, we can write the 2-point correlation function,

$$\xi(\mathbf{r}) = \langle \delta(\mathbf{x}) \delta(\mathbf{x} + \mathbf{r}) \rangle, \qquad (1)$$

and its Fourier transform, the power spectrum $P(\mathbf{k})$, as

$$\langle \delta(\mathbf{k}) \delta(\mathbf{k}') \rangle = (2\pi)^3 \delta_D(\mathbf{k} + \mathbf{k}') P(\mathbf{k}). \qquad (2)$$

Here δ_D denotes the 3-dimensional Dirac delta function, and we use the Fourier transform convention

$$F(\mathbf{x}) = \int \frac{d^3 k}{(2\pi)^3} \, F(\mathbf{k}) e^{i\mathbf{k}\cdot\mathbf{x}}. \qquad (3)$$

Angle brackets around a cosmological field, e.g. $\langle F \rangle$, signify an ensemble average of that quantity over all possible realizations of our universe; in most cases of interest, ergodicity allows us to replace these ensemble averages with spatial averages over a sufficiently large cosmic volume.

In the Lagrangian approach to cosmological fluid dynamics, one traces the trajectory of an individual fluid element through space and time. For a fluid element located at position $\mathbf{q}$ at some initial time t_0, its position at subsequent times can be written in terms of the Lagrangian displacement field $\mathbf{\Psi}$,

$$\mathbf{x}(\mathbf{q}, t) = \mathbf{q} + \mathbf{\Psi}(\mathbf{q}, t), \qquad (4)$$

where $\mathbf{\Psi}(\mathbf{q}, t_0) = 0$. Every element of the fluid is uniquely labeled by its Lagrangian coordinate $\mathbf{q}$ and the displacement field $\mathbf{\Psi}(\mathbf{q}, t)$ fully specifies the motion of the cosmological fluid. Lagrangian Perturbation Theory (LPT) finds a perturbative solution for the displacement field,

$$\mathbf{\Psi}(\mathbf{q}, t) = \mathbf{\Psi}^{(1)}(\mathbf{q}, t) + \mathbf{\Psi}^{(2)}(\mathbf{q}, t) + \mathbf{\Psi}^{(3)}(\mathbf{q}, t) + \cdots. \qquad (5)$$

The first order solution is the Zel'dovich approximation (Zel'dovich

1970), which shall be the focus of this paper. Henceforth we shall denote $\mathbf{\Psi}^{(1)}$ simply as $\mathbf{\Psi}$:

$$\mathbf{\Psi}(\mathbf{q}) = \int \frac{d^3 k}{(2\pi)^3} \, e^{i\mathbf{k}\cdot\mathbf{q}} \frac{i\mathbf{k}}{k^2} \delta_L(\mathbf{k}), \qquad (6)$$

This formalism makes it particularly easy to include redshift space distortions. In this work we adopt the standard "plane-parallel" or "distant-observer" approximation, in which the line-of-sight direction to each object is taken to be the fixed direction $\hat{z}$. This has been shown to be a good approximation at the level of current observational error bars (e.g., Figure 10 of Samushia, Percival, & Raccanelli 2012 or Figure 8 of Yoo & Seljak 2014). Under this assumption, the position of an object located at true comoving position $\mathbf{x}$, will be mis-identified due to its peculiar velocity along the line-of-sight, as

$$\mathbf{s} = \mathbf{x} + \frac{\hat{z} \cdot \mathbf{v}(\mathbf{x})}{aH} \hat{z}. \qquad (7)$$

Thus including redshift-space distortions requires only a simple additive offset of the displacement field. The peculiar velocity of a fluid element, labeled by its Lagrangian coordinate $\mathbf{q}$, is $\mathbf{v}(\mathbf{q}) = a\dot{\mathbf{\Psi}}(\mathbf{q})$ so in redshift space the apparent displacement of the fluid element is

$$\mathbf{\Psi}^s = \mathbf{\Psi} + \frac{\hat{z} \cdot \dot{\mathbf{\Psi}}}{H} \hat{z}. \qquad (8)$$

To a good approximation the time dependence of the nth order term in Eq. (5) is given by $\mathbf{\Psi}^{(n)} \propto D^n$. Therefore $\dot{\mathbf{\Psi}}^{(n)} = nHf\mathbf{\Psi}^{(n)}$, where $f = d\log D/d\log a$ is the growth rate, often approximated as $f \approx \Omega_m^{0.55}$. Thus, within the Zel'dovich approximation, the mapping to redshift space is achieved via the matrix

$$\Psi_i \to \Psi_i^s = (\delta_{ij} + f\hat{z}_i\hat{z}_j)\Psi_j \qquad (9)$$

which simply multiplies the z-component of the vector by $1 + f$.

Finally we must consider biased tracers of the density field. We begin by considering a local Lagrangian bias model, which posits that the locations of discrete tracers at some late time are determined by the overdensities in the initial matter density field, specifically:

$$\rho_X(\mathbf{q}) = \bar{\rho}_X F[\delta_R(\mathbf{q})]. \qquad (10)$$

Here $\bar{\rho}_X$ is the mean comoving number density of our tracer X and the function $F(\delta)$ is called the Lagrangian bias function. Matsubara (2011) provides an extensive discussion of non-local Lagrangian bias.

The correlation function within the Zel'dovich approximation then follows by elementary manipulations (Bond & Couchman 1988; Fisher & Nusser 1996; Matsubara 2008a,b; Carlson, Reid & White 2013; Wang, Reid & White 2013; Tassev 2014b). We begin by writing

$$1 + \delta_X(\mathbf{x}) = \int d^3 q \, F[\delta_R(\mathbf{q})]\delta_D[\mathbf{x} - \mathbf{q} - \mathbf{\Psi}(\mathbf{q})]. \qquad (11)$$

We now replace the delta function with its Fourier representation, and also introduce the Fourier[2] transform $F(\lambda)$ of $F(\delta)$, so the ex-

---

[1] See Bernardeau et al. (2002) for a comprehensive (though somewhat dated) review of Eulerian perturbation theory.

[2] An alternative route to the same final expressions is to expand $F(\delta_R)$ in powers of δ_R and use the properties of Gaussian integrals. We will use the Fourier methodology since it was also used in Matsubara (2008b); Carlson, Reid & White (2013); Wang, Reid & White (2013).
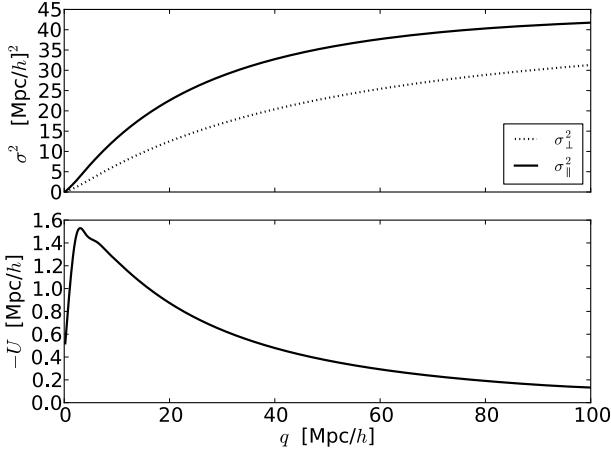
Figure 1. The 2-point functions (Eqs. 23-26) which enter into the computations. The upper panel shows the dispersions, $\sigma_\perp^2 = 2(\sigma_\eta^2 - \eta_\perp)$ and $\sigma_\parallel^2 = 2(\sigma_\eta^2 - \eta_\parallel)$, as a function of q while the lower panel shows the mean velocity, $-U(q)$.

pression for $1 + \delta_X$ becomes

$$1 + \delta_X(\mathbf{x}) = \int d^3 q \, F[\delta_R(\mathbf{q})] \int \frac{d^3 k}{(2\pi)^3} \, e^{i\mathbf{k}\cdot[\mathbf{x}-\mathbf{q}-\mathbf{\Psi}(\mathbf{q})]} \tag{12}$$

$$= \int d^3 q \int \frac{d^3 k}{(2\pi)^3} \int \frac{d\lambda}{2\pi} \, F(\lambda) \, e^{i\{\lambda\delta_R(\mathbf{q})+\mathbf{k}\cdot[\mathbf{x}-\mathbf{q}-\mathbf{\Psi}(\mathbf{q})]\}}. \tag{13}$$

The 2-point correlation function $\xi_X(\mathbf{r}) = \langle \delta_X(\mathbf{x}_1)\delta_X(\mathbf{x}_2)\rangle$ for the biased tracer X is then given by

$$1 + \xi_X(\mathbf{r}) = \int d^3 q_1 \, d^3 q_2 \int \frac{d^3 k_1}{(2\pi)^3} \frac{d^3 k_2}{(2\pi)^3} \, e^{i\mathbf{k}_1\cdot(\mathbf{x}_1-\mathbf{q}_1)} e^{i\mathbf{k}_2\cdot(\mathbf{x}_2-\mathbf{q}_2)}$$
$$\times \int \frac{d\lambda_1}{2\pi}\frac{d\lambda_2}{2\pi} \, F(\lambda_1)F(\lambda_2) \left\langle e^{i[\lambda_1\delta_1+\lambda_2\delta_2-\mathbf{k}_1\cdot\mathbf{\Psi}_1-\mathbf{k}_2\cdot\mathbf{\Psi}_2]}\right\rangle \tag{14}$$

where $\delta_a \equiv \delta_R(\mathbf{q}_a)$, $\mathbf{\Psi}_a \equiv \mathbf{\Psi}(\mathbf{q}_a)$, and $\mathbf{r} = \mathbf{x}_2 - \mathbf{x}_1$. By statistical homogeneity, the expectation value above depends only on the difference in Lagrangian coordinates, $\mathbf{q} = \mathbf{q}_2 - \mathbf{q}_1$. The change of variables $\{\mathbf{q}_1, \mathbf{q}_2\} \to \{\mathbf{q}, \mathbf{Q} = (\mathbf{q}_1 + \mathbf{q}_2)/2\}$ then leads to

$$1 + \xi_X(\mathbf{r}) = \int d^3 q \int \frac{d^3 k}{(2\pi)^3} e^{i\mathbf{k}\cdot(\mathbf{q}-\mathbf{r})} \int \frac{d\lambda_1}{2\pi}\frac{d\lambda_2}{2\pi} \, F_1 F_2 \, K(\mathbf{q}, \mathbf{k}, \lambda_1, \lambda_2), \tag{15}$$

where we have defined

$$K(\mathbf{q}, \mathbf{k}, \lambda_1, \lambda_2) = \left\langle e^{i(\lambda_1\delta_1 + \lambda_2\delta_2 + \mathbf{k}\cdot\mathbf{\Delta})}\right\rangle, \tag{16}$$

and $\mathbf{\Delta} \equiv \mathbf{\Psi}_2 - \mathbf{\Psi}_1$. This expression, derived in Carlson, Reid & White (2013), is the exact configuration space analog of Eq. (9) in Matsubara (2008b) and is analogous to the power spectrum derived in Fisher & Nusser (1996).

We can expand the expectation value in Eq. (16) in terms of cumulants. Since $\delta_R(\mathbf{q})$ and $\mathbf{\Psi}$ are Gaussian only the second cumulant is non-zero

$$\left\langle (\lambda_1\delta_1 + \lambda_2\delta_2 + \mathbf{k}\cdot\mathbf{\Delta})^2\right\rangle_c = (\lambda_1^2 + \lambda_2^2)\sigma_R^2 + A_{ij}k_i k_j$$
$$+ 2\lambda_1\lambda_2\xi_R + 2(\lambda_1 + \lambda_2)U_i k_i, \tag{17}$$

where we have defined

$$\sigma_R^2 = \langle\delta_1^2\rangle_c = \langle\delta_2^2\rangle_c, \qquad \xi_R(\mathbf{q}) = \langle\delta_1\delta_2\rangle_c, \tag{18}$$

$$A_{ij}(\mathbf{q}) = \langle\Delta_i\Delta_j\rangle_c, \qquad U_i(\mathbf{q}) = \langle\delta_1\Delta_i\rangle_c = \langle\delta_2\Delta_i\rangle_c. \tag{19}$$

Eq. (16) then evaluates to

$$K = \exp\left[-\frac{1}{2}(\lambda_1^2 + \lambda_2^2)\sigma_R^2 - \frac{1}{2}A_{ij}k_i k_j - \lambda_1\lambda_2\xi_R - (\lambda_1 + \lambda_2)U_i k_i\right]. \tag{20}$$

This expression is exact, within the Zel'dovich approximation. The quantity σ_R^2 is simply the variance of the smoothed linear density field, while $\xi_R(\mathbf{q}) = \langle\delta_R(\mathbf{q}_1)\delta_R(\mathbf{q}_2)\rangle$ is the corresponding smoothed linear correlation function. The matrix A_{ij} may be decomposed as

$$A_{ij}(\mathbf{q}) = 2\left[\sigma_\eta^2 - \eta_\perp(q)\right]\delta_{ij} + 2\left[\eta_\perp(q) - \eta_\parallel(q)\right]\hat{q}_i\hat{q}_j, \tag{21}$$

$$= \sigma_\perp^2\delta_{ij} + \left[\sigma_\parallel^2 - \sigma_\perp^2\right]\hat{q}_i\hat{q}_j \tag{22}$$

where $\sigma_\eta^2 \equiv \frac{1}{3}\langle|\mathbf{\Psi}|^2\rangle$ is the 1-D dispersion of the displacement field, and $\eta_\parallel$ and $\eta_\perp$ are the transverse and longitudinal components of the Lagrangian 2-point function, $\eta_{ij}(\mathbf{q}) = \left\langle\Psi_i(\mathbf{q}_1)\Psi_j(\mathbf{q}_2)\right\rangle$. The vector $U_i(\mathbf{q}) = U(q)\hat{q}_i$ is the cross-correlation between the linear density field and the Lagrangian displacement field. In the Zel'dovich approximation these quantities are given by

$$\sigma_\eta^2 = \frac{1}{6\pi^2}\int_0^\infty dk \, P_L(k), \tag{23}$$

$$\eta_\perp(q) = \frac{1}{2\pi^2}\int_0^\infty dk \, P_L(k) \, \frac{j_1(kq)}{kq}, \tag{24}$$

$$\eta_\parallel(q) = \frac{1}{2\pi^2}\int_0^\infty dk \, P_L(k) \left[j_0(kq) - 2\frac{j_1(kq)}{kq}\right], \tag{25}$$

$$U(q) = -\frac{1}{2\pi^2}\int_0^\infty dk \, kP_L(k) \, j_1(kq). \tag{26}$$

and shown in Fig. 1. Up to factors of 2 and f, these expressions are identical to the Eulerian velocity correlators in linear theory (e.g. Gorski 1988; Fisher 1995; Reid & White 2011), which is not surprising since $\mathbf{v}_L = f\mathbf{\Psi}$ in the Zel'dovich approximation. It is also useful to define $\sigma_{12}^2 = 2[\sigma_\eta^2 - \mu^2\eta_\parallel - (1 - \mu^2)\eta_\perp]$, the pairwise velocity dispersion at an angle μ to the line-of-sight with the line-of-sight and perpendicular components $\sigma_\parallel^2$ and $\sigma_\perp^2$.

3   CORRELATION FUNCTION – MATTER

For the unbiased case (i.e. the matter field) we can write our expression for $\xi^{(ZA)}$ in closed form by carrying out the Gaussian integral

$$1 + \xi^{(ZA)}(\mathbf{r}) = \int d^3 q \int \frac{d^3 k}{(2\pi)^3} e^{i\mathbf{k}\cdot(\mathbf{q}-\mathbf{r})} e^{-\frac{1}{2}A_{ij}k_i k_j} \tag{27}$$

$$= \int \frac{d^3 q}{(2\pi)^{3/2}|A|^{1/2}} e^{-\frac{1}{2}(\mathbf{r}-\mathbf{q})^\top A^{-1}(\mathbf{r}-\mathbf{q})}, \tag{28}$$

Further discussion of this expression, and the approach to linear theory, can be found in Carlson, Reid & White (2013).

Evaluation of $\xi^{(ZA)}$ involves a numerical integral of a Gaussian function. The inversion of A_{ij} which is required can be done analytically by use of the Sherman-Morrison formula which states that for matrices M and vectors b and c,

$$\left(M + bc^T\right)^{-1} = M^{-1} - \frac{M^{-1}bc^T M^{-1}}{1 + c^T M^{-1}b}. \tag{29}$$

Writing $A_{ij} = F\delta_{ij} + G\,\widehat{q_i}\widehat{q_j}$ (see Eq. 22) we have

$$A_{ij}^{-1} = \frac{\delta_{ij}}{F} - \frac{G\,\widehat{q_i}\widehat{q_j}}{F(F + G)} \tag{30}$$

$$= \frac{\delta_{ij}}{\sigma_\perp^2} + \frac{\sigma_\perp^2 - \sigma_\parallel^2}{\sigma_\parallel^2\sigma_\perp^2}\hat{q}_i\hat{q}_j \tag{31}$$

where $F = \sigma_\perp^2$, $G = \sigma_\parallel^2 - \sigma_\perp^2$ and the combination $F + G = \sigma_\parallel^2$.

To compute the determinant we make use of $\det(cM) = c^3\det M$ for scalar c and 3×3 matrix M and that $\det(I + uv^T) = 1 + u^T v$. Then

$$\det A = \left(\sigma_\perp^2 \sigma_\parallel\right)^2 \qquad (32)$$

as expected. The integrand can thus be expressed analytically in terms of the 2-point functions defined previously and evaluated by simple quadratures[3] in $\mathbf{x} = \mathbf{q} - \mathbf{r}$. The integral is dominated by $\mathbf{q} \approx \mathbf{r}$. By tabulating the functions $\eta_i(q)$ and $U(q)$ in advance these integrals can be performed very quickly. In redshift space we replace

$$U_i \rightarrow U_i^s = (\delta_{ij} + f\hat{z}_i\hat{z}_j)U_j, \qquad (33)$$
$$A_{ij} \rightarrow A_{ij}^s = (\delta_{ik} + f\hat{z}_i\hat{z}_k)(\delta_{jl} + f\hat{z}_j\hat{z}_l)A_{kl}. \qquad (34)$$

This corresponds simply to dividing the z-components of the inverse of A by $1 + f$ and multiplying U_z by $1 + f$.

4   PERTURBATIVE EXPANSION FOR BIASED TRACERS

Returning to the case of biased tracers, consider again Eq. (20). In the unbiased case the $\mathbf{k}$ integration in Eq. (15) took the form of a Gaussian integral, which we carried out analytically. In the biased case, we can achieve the same thing if we first partially expand Eq. (20) as

$$
\begin{aligned}
K = {} & e^{-\frac{1}{2}(\lambda_1^2 + \lambda_2^2)\sigma_R^2}e^{-\frac{1}{2}\mathbf{k}^T A\mathbf{k}}\Big[1 - (\lambda_1 + \lambda_2)U_ik_i - \lambda_1\lambda_2\xi_R \\
& + \frac{1}{2}(\lambda_1 + \lambda_2)^2 U_iU_jk_ik_j + \lambda_1\lambda_2(\lambda_1 + \lambda_2)\xi_R U_ik_i + \frac{1}{2}\lambda_1^2\lambda_2^2\xi_R^2 \\
& - \frac{\lambda_1^3\lambda_2^3}{3!}\xi_R^3 - \frac{1}{2}\lambda_1\lambda_2(\lambda_1 + \lambda_2)^2 U_iU_jk_ik_j\xi_R \\
& - \frac{1}{2}\lambda_1^2\lambda_2^2(\lambda_1 + \lambda_2)U_ik_i\xi_R^2 - \frac{(\lambda_1 + \lambda_2)^3}{3!}U_iU_jU_nk_ik_jk_n \\
& + \frac{\lambda_1^4\lambda_2^4}{4!}\xi_R^4 + \cdots\Big]
\end{aligned}
\qquad (35)
$$

We may justify this choice of expansion by noting that both $\xi_R(\mathbf{q})$ and $U_i(\mathbf{q})$ vanish in the large-scale limit $|\mathbf{q}| \rightarrow \infty$, while σ_R^2 and $A_{ij}(\mathbf{q})$ approach non-zero values. At this stage we note one difference between doing this expansion within Lagrangian perturbation theory (e.g. Matsubara 2008b; Okamura, Taruya, & Matsubara 2011; Carlson, Reid & White 2013) and performing it within the context of the Zel'dovich expansion. In the Zel'dovich approximation all the terms are just multiples of 2-point functions and we can go to arbitrarily high order without the need to evaluate any high dimensional mode coupling integrals or numerically difficult terms. Here we have gone to cubic order in the 2-point function and indicated how the quartic terms appear. We shall show later that the expansion seems to be converging quickly.

The λ_1 and λ_2 integrations give $(-i)^n\left\langle F^{(n)}\right\rangle$, the expectation value of the nth derivative of the Lagrangian bias function $F(\delta)$ (Matsubara 2008b). In order to make the expressions more readable

we shall write $b_n = \left\langle F^{(n)}\right\rangle$. Then

$$
\begin{aligned}
L(\mathbf{q}, \mathbf{k}) \equiv {} & \int \frac{d\lambda_1}{2\pi}\frac{d\lambda_2}{2\pi}\, F(\lambda_1)F(\lambda_2)\, K(\mathbf{q}, \mathbf{k}, \lambda_1, \lambda_2) \qquad (36) \\
= {} & e^{-\frac{1}{2}A_{ij}k_ik_j}\Big[1 + b_1^2\xi_R + 2ib_1U_ik_i + \frac{1}{2}b_2^2\xi_R^2 \\
& - (b_2 + b_1^2)U_iU_jk_ik_j + 2ib_1b_2\xi_R U_ik_i \\
& + \frac{b_3^2}{3!}\xi_R^3 - (b_1b_3 + b_2^2)U_iU_jk_ik_j\xi_R \\
& + ib_2b_3U_ik_i\xi_R^2 - i(b_1b_2 + \frac{1}{3}b_3)U_iU_jU_nk_ik_jk_n \\
& + \cdots\Big].
\end{aligned}
\qquad (37)
$$

The $\mathbf{k}$ integration reduces to a series of multi-variate Gaussian integrals which can be done with the formulae in Carlson, Reid & White (2013). In the end we obtain

$$
\begin{aligned}
M(\mathbf{r}, \mathbf{q}) \equiv {} & \int \frac{d^3k}{(2\pi)^3}\, e^{i\mathbf{k}\cdot(\mathbf{q}-\mathbf{r})}L(\mathbf{q}, \mathbf{k}) \qquad (38) \\
= {} & \frac{1}{(2\pi)^{3/2}|A|^{1/2}}\, e^{-\frac{1}{2}(\mathbf{r}-\mathbf{q})^T A^{-1}(\mathbf{r}-\mathbf{q})}\Big[1 + b_1^2\xi_R \\
& - 2b_1U_ig_i + \frac{1}{2}b_2^2\xi_R^2 - (b_2 + b_1^2)U_iU_jG_{ij} \\
& - 2b_1b_2\xi_R U_ig_i + \frac{b_3^2}{3!}\xi_R^3 - (b_1b_3 + b_2^2)G_{ij}U_iU_j\xi_R \\
& - b_2b_3U_ig_i\xi_R^2 + (b_1b_2 + \frac{1}{3}b_3)\Gamma_{ijn}U_iU_jU_n \\
& + \cdots\Big],
\end{aligned}
\qquad (39)
$$

where

$$
\begin{aligned}
g_i &\equiv (A^{-1})_{ij}(q - r)_j \\
G_{ij} &\equiv (A^{-1})_{ij} - g_ig_j \\
\Gamma_{ijk} &\equiv (A^{-1})_{ij}g_k + (A^{-1})_{ki}g_j + (A^{-1})_{jk}g_i - g_ig_jg_k
\end{aligned}
\qquad (40)
$$

so that

$$\Gamma_{ijn}U_iU_jU_n = 3\left(U_iG_{ij}U_j\right)(U_ng_n) + 2\left(U_ig_i\right)^3 \qquad (41)$$

Our final expression for the correlation function is

$$1 + \xi_X(\mathbf{r}) = \int d^3q\, M(\mathbf{r}, \mathbf{q}). \qquad (42)$$

The remaining integration over $\mathbf{q}$ must be performed numerically as before.

One can treat the b_n as fitting parameters, or attempt to compute them from a bias model. One such model is the peak-background split, which begins with the unconditional multiplicity function

$$\nu f(\nu)\, d\nu = \frac{M}{2\bar{\rho}}\frac{dn}{dM}\, dM \qquad (43)$$

which can be fit with

$$\nu f(\nu) \propto \left(1 + \frac{1}{(a\nu^2)^p}\right)\left(\frac{a\nu^2}{2}\right)^{1/2}\exp\left(-\frac{a\nu^2}{2}\right) \qquad (44)$$

where $a = 1$, $p = 0$ gives the Press-Schecter mass function (Press & Schechter 1974), while $a = 0.707$, $p = 0.3$ yields the Sheth-Tormen mass function (Sheth & Tormen 1999). Within the assumption of the peak-background split, the conditional multiplicity function is given by the substitution,

$$\nu \rightarrow \nu\left(1 - \frac{\delta}{\delta_c}\right), \qquad (45)$$

---

[3] We use the midpoint rule in $|\mathbf{q} - \mathbf{r}|$ and Gauss-Legendre integration in $\widehat{q \cdot r}$.
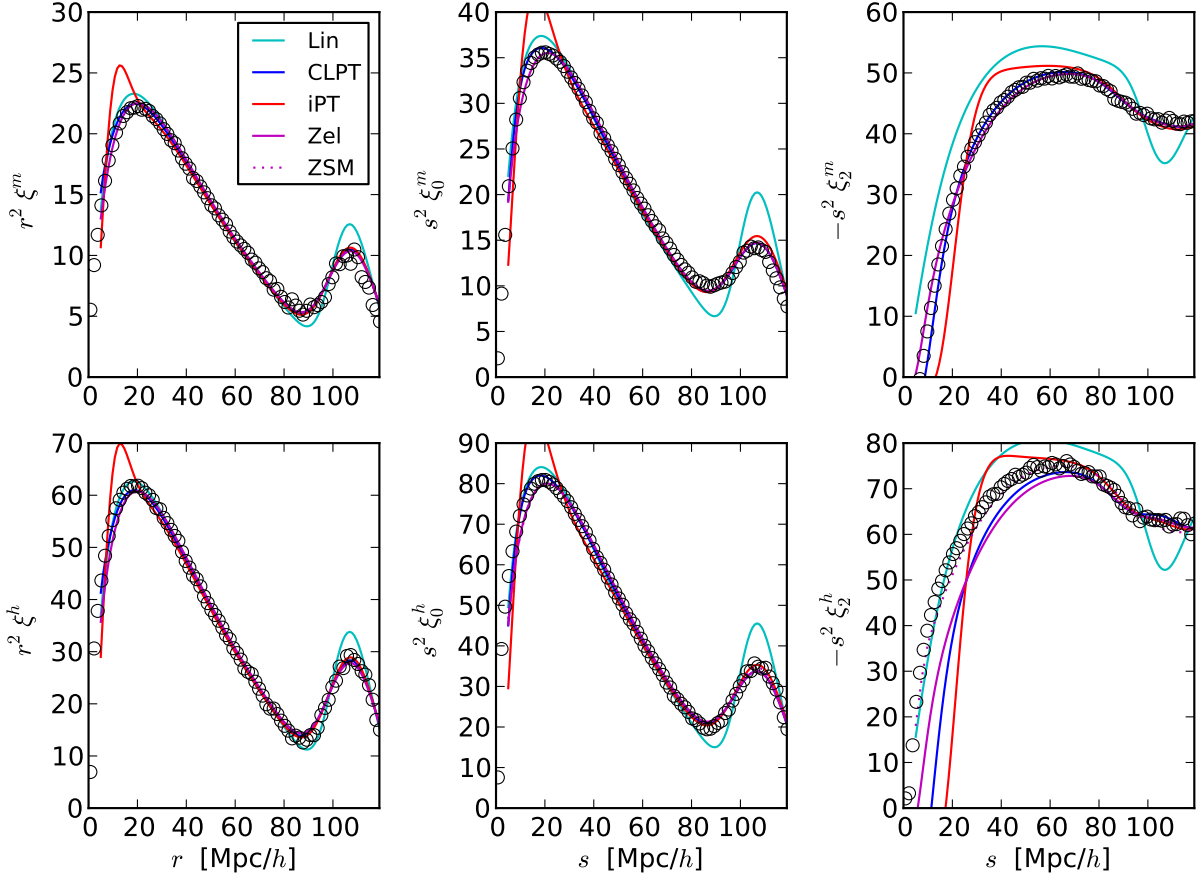
Figure 2. A comparison of different Lagrangian perturbative schemes to N-body results for the 2-point function, ξ, in real- and redshift-space. The results are for the cosmology used in Carlson, Reid & White (2013), which has $\Omega_m = 0.274$, at $z = 0.55$. The points show the average over 20 realizations of the N-body simulation while the lines show the analytic approximations: linear theory (cyan); convolution Lagrangian perturbation theory (CLPT; Carlson, Reid & White 2013, blue); integrated perturbation theory (iPT; Matsubara 2008b, red); the Zel'dovich approximation (magenta) and the Zel'dovich streaming model (ZSM; dotted magenta). The upper row is for the matter, while the lower row is for biased tracers with $b \simeq 1.6$ (friends-of-friends halos with $12.785 < \log_{10} M_h/(h^{-1}M_\odot) < 13.085$). From left to right the columns are the real-space correlation function, the redshift-space monopole and the redshift-space quadrupole, all multiplied by r^2 to allow a linear y-axis. Note that the Zel'dovich approximation provides a good fit to the N-body data on large scales for all but the quadrupole moment of the redshift-space halo correlation function (lower right panel). The fact that the iPT, CLPT and Zel'dovich lines are almost indistinguishable on large scales shows the good convergence of Lagrangian perturbation theory schemes.

where δ is the background density and $\delta_c \simeq 1.686$ is the critical overdensity for collapse. The Lagrangian bias parameters then follow from Taylor expanding the (appropriately normalized) conditional multiplicity function as a function of δ, yielding $b_n = [\nu f(\nu)]^{-1} d^n/d\delta^n[\nu f(\nu)]$ or

$$b_1(\nu) = \frac{1}{\delta_c}\left[a\nu^2 - 1 + \frac{2p}{1 + (a\nu^2)^p} \right], \qquad (46)$$

$$b_2(\nu) = \frac{1}{\delta_c^2}\left[a^2\nu^4 - 3a\nu^2 + \frac{2p(2a\nu^2 + 2p - 1)}{1 + (a\nu^2)^p} \right], \qquad (47)$$

and

$$
b_3(\nu) = \frac{1}{\delta_c^3}\Big[a^3\nu^6 - 6a^2\nu^4 + 3a\nu^2 +
$$
$$
+ \frac{2p(3a^2\nu^4 + 6a\nu^2(p-1) + 4p^2 - 1)}{1 + (a\nu^2)^p} \Big] . \qquad (48)
$$

For the halo sample shown in Fig. 2 we have $\nu \simeq 1.6$, $b_1 = 0.64$,

$b_2 = -0.45$ and $b_3 = -1.63$ from the Sheth-Tormen mass function and we have used these values in the relevant figures. There is some evidence (Baldauf et al. 2012) that simplistic bias models such as the above are not quantitatively accurate when compared to N-body simulations. On large scales the level of agreement is quite insensitive to the value assumed for $b_{n\geqslant 2}$ as long as $|b_{n\geqslant 2}|$ is not much larger than b_1 because the terms involving $b_{n\geqslant 2}$ are numerically small compared to the b_1 terms. Thus assuming the peak-background split value for $b_{n\geqslant 2}$ is perfectly adequate and in matching the Zel'dovich theory to observations there is only one free parameter (ν or b_1). This is very well constrained by the overall amplitude of ξ.

5 RESULTS

Figs. 2 and 3 compare the predictions of the Zel'dovich approximation to a number of other Lagrangian perturbation theory schemes
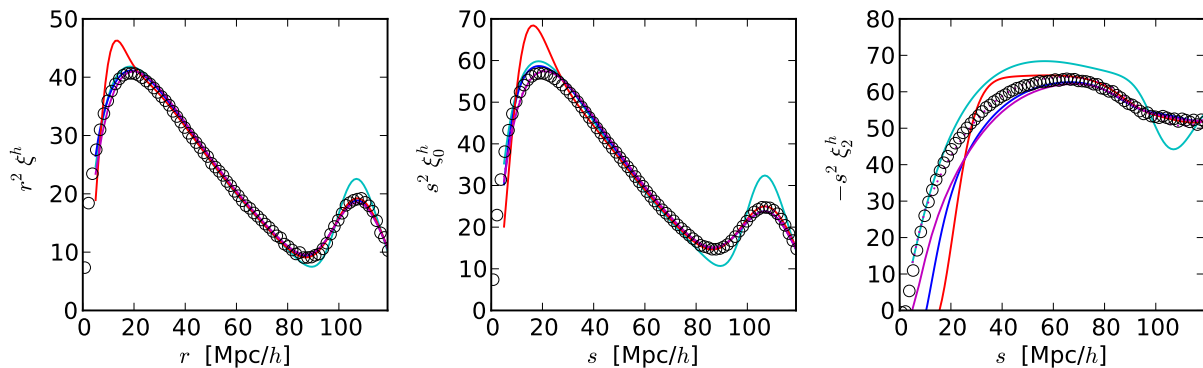
Figure 3. As for Fig. 2 except for a different halo mass range. The panels and line types are the same as the lower three panels of Fig. 2 but for friends-of-friends halos with $12.182 < \log_{10} M_h/(h^{-1}M_\odot) < 12.483$ with large-scale bias $b \simeq 1.3$.

and to the clustering of halos in an N-body simulation. The agreement between the predictions of the Zel'dovich approximation and N-body simulations is very good on large scales. For the real-space correlation function and the redshift-space monopole the agreement extends down to $10 - 20\,h^{-1}$Mpc for both the matter and halos. However, the theory does much less well for the halo quadrupole (a problem shared with all of the local Lagrangian bias schemes shown in Fig. 2). One major difference between the halo calculation and the matter calculation is the Taylor series expansion of the bias terms.

While the perturbative schemes plotted in Fig. 2 stop at $O(P_L^2)$, we have extended the Zel'dovich calculation one additional order to see if the higher order terms could contribute to the quadrupole on intermediate and small scales. We find that the terms cubic in ξ_R and U contribute negligibly to the real-space correlation function and the monopole and quadrupole moments of the redshift-space correlation function for $r > 10\,h^{-1}$Mpc. Since the $O(P_L^3)$ terms do not contribute significantly to any of the statistics for this halo sample it appears that the Taylor series expansion is not the source of the discrepancy. This also suggests that truncating the expansion at $O(P_L^2)$ is a good approximation and that the expansion is converging. Henceforth we shall drop the $O(P_L^3)$ terms.

The contribution to the correlation functions is not shared equally among the terms. Working above $r = 10\,h^{-1}$Mpc we find that the real-space correlation function is dominated by the $U_i g_i$, "1" and ξ_R terms in the square brackets of Eq. (39). The redshift-space monopole is dominated by the same three terms. Fig. 4 shows how the different terms contribute to the final peak in $s^2 \xi_0^h(s)$ near $110\,h^{-1}$Mpc and to the quadrupole. Above $50\,h^{-1}$Mpc the terms "1" and $U_i g_i$ in the square brackets in Eq. (39) contribute the vast majority of the total quadrupole signal, with approximately equal contributions. By $20\,h^{-1}$Mpc the other terms contribute about 10 per cent of the total, with the $U_i U_j G_{ij}$, $U_i g_i \xi_R$ and ξ_R terms contributing the remainder in decreasing order of importance (the ξ_R^2 term provides a negligible contribution).

Fig. 5 shows the degree to which the b_1 and b_2 terms depend on scale differently than the matter terms. In all cases, above $10\,h^{-1}$Mpc the level of scale-dependence is quite small. The actual shape of the real-space correlation function and the redshift-space monopole correlation function differ at the ten per cent level near the peak, but this difference is due to the impact of redshift space distortions on the correlation function and not due to scale-

dependent bias in the sense that we mean it here. Note that this relative scale-independence does not need to hold in Fourier space. As a trivial example, $P(k) = b^2 P_L(k) + N(k)$ has a scale-independent configuration-space bias if the transform of $N(k)$ is arbitrarily small on the scales of interest. Taking $N(k) = \bar{n}^{-1}$, $N(k) \propto \exp[-k^2 R^2]$ or the convolution of two halo profiles can satisfy this criterion. Depending on the size of $N(k)/P_L(k)$ this could lead to a large (but smoothly varying) scale-dependent bias in Fourier space (see e.g. the discussion in Schulz & White 2006). Conversely, one finds that the Fourier transform of the Zel'dovich correlation function has almost no power beyond $k \sim \sigma_\eta^{-1}$. To use the Zel'dovich approximation in Fourier space requires the addition of other terms which provide the missing power but affect the correlation function only at small scales.

Interestingly, the Zel'dovich approximation predicts that halos which are locally biased in Lagrangian space will have approximately the same small-scale quadrupole to large-scale quadrupole ratio as the matter, while the halos in N-body simulations display a significantly larger small-scale quadrupole when scaled to the same large-scale quadrupole. The term involving b_2 gives the desired increase in small-scale quadrupole, though at too small an amplitude. Making b_2 large and positive helps slightly, but the quadrupole still has the wrong overall shape.

Some authors (e.g. Melott, Pellman & Shandarin 1994) have suggested that the Zel'dovich approximation performs better when small-scale power is filtered out of the linear theory power spectrum. We have tested this by Gaussian filtering the input $P_L(k)$ on scales $1 - 5\,h^{-1}$Mpc. We find that none of these scales improves the agreement of the quadrupole of the redshift-space correlation function on smaller scales.

At this point it is unclear whether the discrepancy above is due to our assumption of local Lagrangian bias or the Zel'dovich dynamics predicting the wrong velocity field for halos. To explore this issue further, we have run another set of 8 simulations with a simplified set-up. Each simulation started with initial conditions generated with the Zel'dovich approximation at $z_{ic} = 67$ (where the rms displacement was about 10 per cent of the inter-particle spacing). To ensure numerical convergence we smoothed the linear power spectrum with a Gaussian of $1\,h^{-1}$Mpc. Again 1500^3 particles in a $1.5\,h^{-1}$Gpc box were employed and for each particle, the value of the initial density, evaluated on the 1500^3 grid, was stored. The particles were integrated to $z \simeq 0.55$ either using a particle-
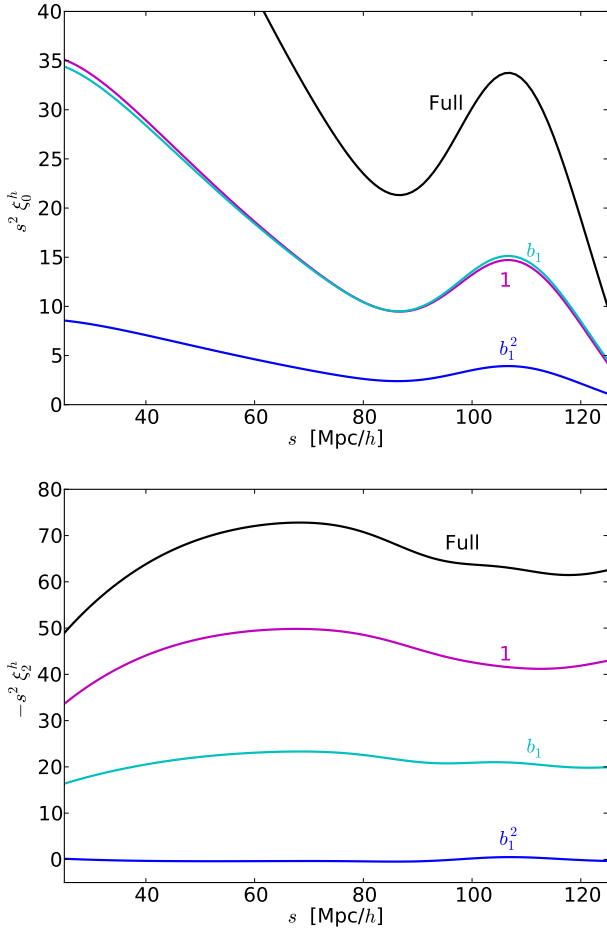
Figure 4. (Top) The peak in $s^2\xi_0^h(s)$ near $110\,h^{-1}$Mpc and the contributions from the various terms. The black line shows the full Zel'dovich prediction, which is is indistinguishable from the prediction with $b_2 = 0$. The magenta line shows the contribution from the "1" term in Eq. (39). The cyan line shows the contribution from the term linear in b_1 and the blue line the term quadratic in b_1. (Bottom) The same for the quadrupole, $-s^2\xi_2^h(s)$.

mesh (PM) code (with a 1500^3 mesh) or the Zel'dovich approximation. Particles were then selected if their density field in the initial conditions (extrapolated to $z = 0$ using linear theory) exceeded some threshold. In this manner the simulations mimic the analytic calculation closely.

In the analytic calculation we also used a linear theory power spectrum smoothed with a $1\,h^{-1}$Mpc Gaussian, and we set b_n assuming $F(\delta) \propto \Theta(\delta - \delta_c)$, i.e.

$$b_1 = \sqrt{\frac{2}{\pi}}\left[\sigma\,\mathrm{erfc}\left(\frac{\delta_c}{\sqrt{2}\,\sigma}\right)\right]^{-1} e^{-\delta_c^2/2\sigma^2} \to \frac{\delta_c}{\sigma^2} \quad (49)$$

$$b_2 = \sqrt{\frac{2}{\pi}}\left[\frac{\sigma^3}{\delta_c}\,\mathrm{erfc}\left(\frac{\delta_c}{\sqrt{2}\,\sigma}\right)\right]^{-1} e^{-\delta_c^2/2\sigma^2} \to \frac{\delta_c^2}{\sigma^4} \quad (50)$$

(Szalay 1988; Matsubara 2011) where the limits shown are for $\delta_c \gg 1$ and can be compared to the leading order behavior in Eqs. (46, 47) with $\nu = \delta_c/\sigma$. We have chosen δ_c such that the large-scale bias is approximately 1.6, as for the halo sample in Fig. 2.

Fig. 6 shows the real-space correlation function and the monopole and quadrupole moments of the redshift-space correlation function for all three methods, focusing on intermediate scales.
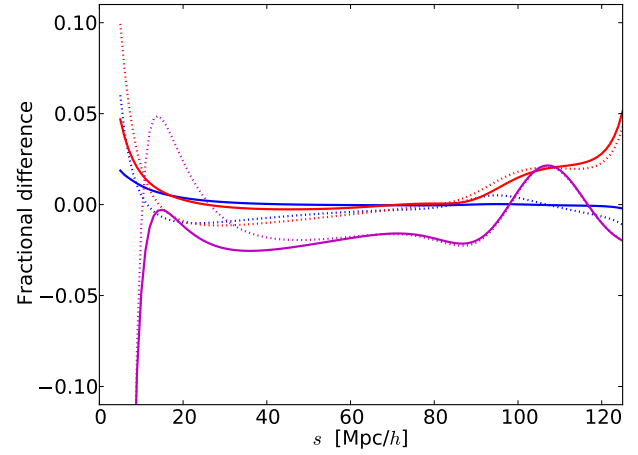
Figure 5. The fractional difference between the full Zel'dovich calculation for the halo real-space correlation function (blue), redshift-space monopole (red) and quadrupole (magenta) and the 'constant bias' approximations: $(1+b_1)^2\xi^m$, $(1+b_1)^2(1+[2/3]\beta+[1/5]\beta^2)/(1+[2/3]f+[1]5/f^2)\xi_0^m$ and $[b/3+f/7]/[1/3+f/7]\xi_2^m$. Here $\beta \equiv f/(1+b_1)$ and $f \approx 0.744$ for this cosmology and redshift. The solid lines include all of the terms, while the dotted lines show the computation with $b_2 = 0$.

The lower curves/points show the results for the matter field while the upper curves/points show the results for all particles with initial δ above a threshold. Note that there are no free parameters in this comparison! The agreement between the N-body results, the Zel'dovich simulations and the theory is excellent for the real-space correlation function and the monopole of the redshift-space correlation function. The agreement remains good (though not perfect) for the quadrupole of the matter field, but is less good for particles selected by initial density. In particular the PM results show the same qualitative difference from the Zel'dovich results as was found in the TreePM runs with halos. This suggests that the mismatch in the halo quadrupole that we are seeing in Figs. 2 and 3 is at least partly due to inadequacies in the Zel'dovich prediction for the inter-halo relative velocities (see also Seto & Yokoyama 1998; Tassev & Zaldarriaga 2012b,c), though some may be due to our assumption of local Lagrangian bias. We discuss non-local bias next.

6 BEYOND LOCAL BIAS

The failure of our model to match the quadrupole moment on small and intermediate scales may be due in part to our assumption of local Lagrangian bias. While this approximation has received support from N-body simulations (Roth & Porciani 2011; Baldauf et al. 2012; Chan, Scoccimarro, & Sheth 2012; Wang & Szalay 2012) it must break down at some level.

Perhaps the simplest modification to our formalism would be to allow a q-dependence to the bias coefficients, b_n. For example we could consider $b_1 \to b_1[1 + q_\star^2/q^2]$. For suitably chosen $q_\star$, such a modification can improve the agreement of the quadrupole at intermediate scales ($s \approx 50\,h^{-1}$Mpc) but it changes the monopole in a manner qualitatively similar to the overshoot seen in iPT in Fig. 2. In general a large enough modification to create agreement for the quadrupole removes the good agreement with the monopole. However it is possible to adjust $q_\star$ so that the disagreement for the monopole is on small scales ($s < 30\,h^{-1}$Mpc) while the agreement for the quadrupole is improved non-negligbly over the range $30 <$
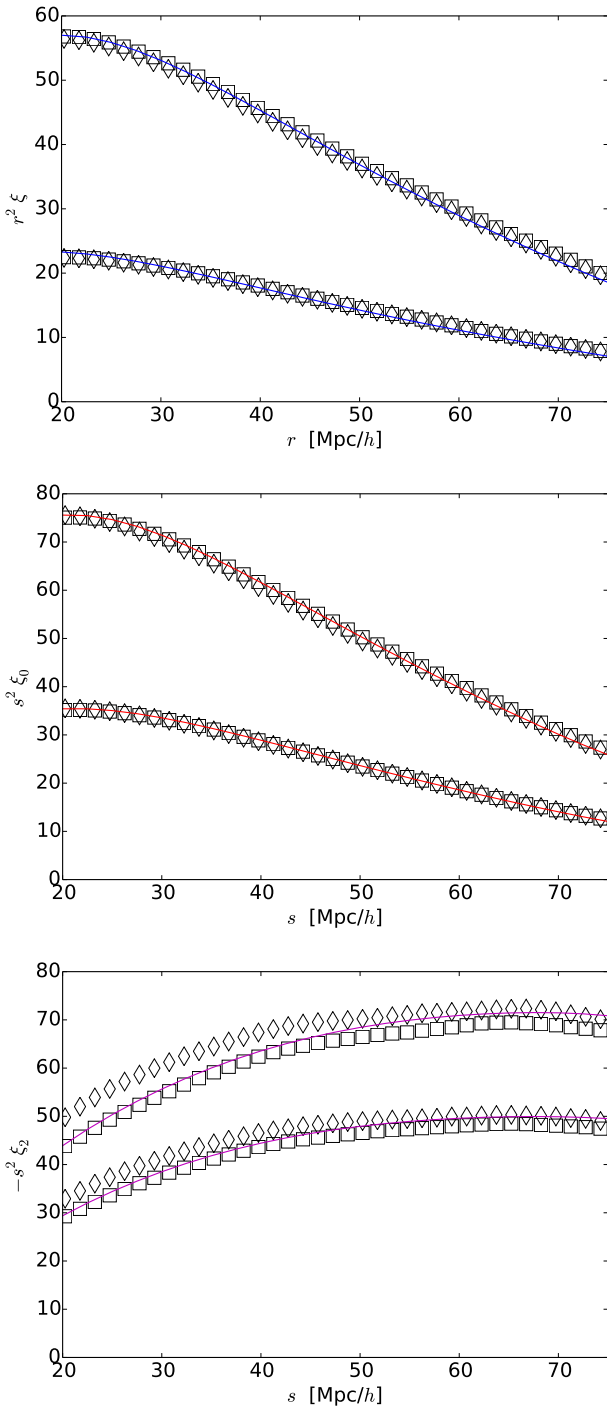
Figure 6. The real-space correlation function (top) and the monopole (middle) and quadrupole (bottom) moments of the redshift-space correlation function for our simulations based on thresholding. In each panel the lines represent the analytic model, the squares the results of the Zel'dovich simulations and the diamonds the results of the PM simulations. The upper curves/points are for points with $\delta_{\rm lin}$ above a threshold while the lower curves/points are for all $\delta_{\rm lin}$. There are no free parameters in this comparison! Note that the quadrupole moment is more sensitive to the full nonlinear evolution than either the monopole or real-space correlation function.

$s < 75\,h^{-1}{\rm Mpc}$. Indeed, by "softening" the bias using a form like $b_1 \to b_1[1+q_\star^2/(q^2+\varepsilon^2)]$ both the monopole and quadrupole can be made to agree with the N-body results to better than 5 per cent for $s > 30\,h^{-1}{\rm Mpc}$, though the theory rapidly departs from the N-body results for smaller scales.

We also expect that terms involving e.g. the tidal tensor, can become important for high mass halos (Sheth, Chan & Scoccimarro 2012). Such terms are naturally quadrupolar in nature and may affect the predictions. While shear terms are naturally induced by gravitational evolution, here we are interested in any dependence in the initial conditions.

Suppose we extend $F(\delta)$ to also include a tidal-shear dependence, $F(\delta, s^2)$, as discussed for example by McDonald & Roy (2009)? We can Fourier transform on s^2 as well, generating a term $\exp[i\zeta s^2]$. Since $s^2 = s_{ij}s_{ij}$, with

$$s_{ij}(\mathbf{k}) = \left(\frac{k_i k_j}{k^2} - \frac{1}{3}\delta_{ij}\right)\delta(\mathbf{k}) \qquad (51)$$

is already quadratic in δ, in the exponential it appears[4] only multiplied by other expectation values. Throughout we shall subtract the mean, $\langle s^2\rangle = (2/3)\langle\delta^2\rangle$, from s^2. Working to lowest order in ζ the additional terms to be added inside the $[\cdots]$ in Eq. (35) go as

$$\left\langle s_1^2 s_2^2\right\rangle \quad,\quad \left\langle s^2\delta^2\right\rangle \quad,\quad \left\langle s^2\delta\Psi\right\rangle \quad,\quad \left\langle s^2\mathbf{\Psi}^2\right\rangle \qquad (52)$$

since the other terms involve the expectation value of an odd number of Gaussian fields. The relevant formulae can be found in the appendix. The terms are shear-density correlations: $-i[\zeta_1\lambda_2^2+\zeta_2\lambda_1^2]\left\langle s_{ij}(\mathbf{q}_1)\delta(\mathbf{q}_2)\right\rangle^2$; shear-shear terms: $-(\zeta_1^2+\zeta_2^2)\langle s^2\rangle$ and $-\zeta_1\zeta_2\langle s_1 s_2\rangle^2$; shear-displacement terms: $(\zeta_1+\zeta_2)\langle s_{ij}(\mathbf{q}_1)k_m\Psi_m(\mathbf{q}_2)\rangle^2$ and cross-terms $-2i(\zeta_1\lambda_2 + \zeta_2\lambda_1)\langle s_{ij}(\mathbf{q}_1)\delta(\mathbf{q}_2)\rangle\langle s_{ij}(\mathbf{q}_1)k_m\Psi_m(\mathbf{q}_2)\rangle$. These last terms include contributions with $\hat{k}\cdot\hat{q}$ and $(\hat{k}\cdot\hat{q})^2$ into Eq. (37) and appear to be the best bet for influencing the quadrupole.

The terms involving s^2 are very small, as expected since they are higher order in P_L. Even allowing for arbitrary prefactors in front of the terms, the halo quadrupole cannot be matched without spoiling the agreement with the redshift-space monopole and real-space correlation function. This is because the terms which enter contribute approximately the same amount to the monopole as to the quadrupole (as was the case with the non-shear terms). It thus appears that the lack of shear terms in the bias function is not the reason for the discrepancy seen in Fig. 2.

One may take a more general approach. Within the context of the Zel'dovich approximation, the terms appearing in the square brackets in Eq. (37) will be functions of q and will be contracted with various factors of $\mathbf{k}$. There will be scalars, like ξ_R, vectors, like $\mathbf{U}$, and tensors of various ranks. The vectors must be proportional to $\hat{q}_i$. The rank-2 tensors must go as a sum of terms like δ_{ij} and $\hat{q}_i\hat{q}_j$, and similarly for higher rank objects. The most general biasing scheme would therefore consist of all such terms, with general dependence on q. We have not undertaken an exploration of this large parameter space, but our experience above suggests that any such terms will contribute approximately equally to the monopole and the quadrupole moment, making it difficult to substantially adjust the quadrupole on small scales without spoiling the agreement seen for the monopole. As we saw above when we modified $b_1 \to b_1(1 + q_\star^2/q^2)$, it is possible to improve the level of agreement in some cases, though we do not posses a theory which predicts the required functional form at present.

---

[4] When using the cumulant theorem, bear in mind that s^2 is not Gaussian.

On the basis of these investigations it appears that the disagreement between the Zel'dovich prediction for the quadrupole moment of the redshift-space, halo correlation function and that measured in N-body simulations may be due to simplifications inherent in the Zel'dovich approximation itself. Perhaps the relative velocities predicted from the lowest order displacement field are not as accurate for larger δ_L. Consistent with this view, we note that CLPT (which goes to next order in Lagrangian perturbation theory) does perform (very slightly) better than the Zel'dovich approximation in the range $40 < s < 70 \, h^{-1}\text{Mpc}$. Higher order LPT calculations are also known to give more accurate values for the moments (e.g. Munshi, Sahni & Starobinsky 1994). However, the convergence appears to be very slow at best.

7 ZEL'DOVICH STREAMING MODEL (ZSM)

If the pure Zel'dovich calculation cannot match the small-scale quadrupole moment of the halo correlation function, can it be part of an extended model which can? The tests above suggest that the failure of the Zel'dovich approximation lies in the pairwise velocity distribution predicted by the model. Reid & White (2011) showed that the halo pairwise velocity distribution was quite well approximated by a Gaussian. What if we enforce this functional form (the "Gaussian streaming model"), using the Zel'dovich approximation to compute the ingredients: the real-space clustering of biased tracers, the mean infall velocity and the velocity dispersion? Specifically we assume

$$1 + \xi^s(s_\perp, s_\parallel) = \int \frac{dy}{[2\pi]^{1/2}\sigma_{12}} [1 + \xi(r)] \exp\left\{ -\frac{[s_\parallel - y - \mu v_{12}]^2}{2\sigma_{12}^2} \right\},$$
(53)

with $\xi(r)$, v_{12} and σ_{12} from the analytic theory. This expression simply enforces pair counting, assuming that the functional form of the velocity distribution is Gaussian, centered at μv_{12}; the mean LOS velocity between a pair of tracers as a function of their real space separation. We have just shown that the Zel'dovich approximation works well for the real-space correlation function of biased tracers, such as halos. The scale-dependence of the velocity dispersions[5] is well predicted by linear theory (Reid & White 2011; Wang, Reid & White 2013). Thus the only missing ingredient is the mean infall velocity.

We can use the method described in Wang, Reid & White (2013) to compute v_{12} within the Zel'dovich approximation. One simply adds a term $\mathbf{J} \cdot \dot{\boldsymbol{\Delta}}$ to the exponent in Eq. (16) and computes derivatives with respect to $\mathbf{J}$, This is a subset of the calculation presented in Wang, Reid & White (2013):

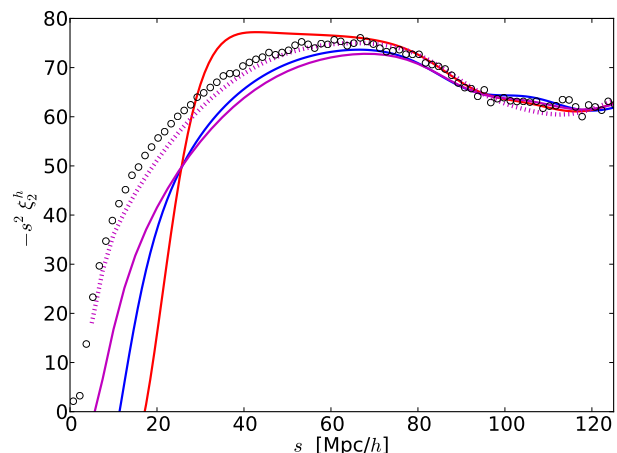$$\mathbf{v}_{12} = [1 + \xi]^{-1} \int d^3q \, \mathbf{M}(\mathbf{r}, \mathbf{q})$$
(54)

Figure 7. The quadrupole moment of the halo correlation function, multiplied by s^2. This is the same as the lower right panel of Fig. 2.

with[6]

$$
\begin{aligned}
M_n &= \frac{f}{(2\pi)^{3/2}|A|^{1/2}} e^{-(1/2)(q_i - r_i)A_{ij}^{-1}(q_j - r_j)} \\
&\times \left\{ -g_i A_{in} + 2b_1 \left[U_n - U_i G_{ij} A_{jn} \right] - 2b_2 g_i U_i U_n \right. \\
&\left. - b_1^2 \left[2g_i U_i U_n + \xi_L g_i A_{in} \right] + 2b_1 b_2 \xi_L U_n \right\},
\end{aligned}
$$
(55)

Note that we are interested in the line-of-sight velocity, so we require only the component of $\mathbf{M}$ along $\mathbf{r}$.

The predictions of the Zel'dovich streaming model (ZSM) are shown in Fig. 2 as the dotted magenta lines. They are indistinguishable from the Zel'dovich model above except for the lower right panel (halo quadrupole). We reproduce the quadrupole results in Fig. 7 where we see the model improves upon the Zel'dovich calculation significantly at small separation, even though it only involves simple, one-dimensional integrals of the linear theory power spectrum. Above $15 \, h^{-1}\text{Mpc}$ the ZSM prediction for the quadrupole is within 10 per cent of the N-body result. Above $30 \, h^{-1}\text{Mpc}$ it is within 5 per cent of the N-body result and above $50 \, h^{-1}\text{Mpc}$ it is within 1 per cent of the N-body result. For the halo sample shown in Fig. 3 the corresponding numbers are 4 per cent, 1 per cent and 1 per cent.

8 DISCUSSION

The Zel'dovich approximation (Zel'dovich 1970) remains one of our most powerful analytic models of large-scale structure. We have presented a derivation of correlation function, in real- and redshift-space, within the Zel'dovich approximation including an analytic inversion of the Lagrangian correlator which appears as the fundamental ingredient of the model. The resulting integral expression is exact within the context of the Zel'dovich approximation and can be rapidly evaluated using quadratures. We have compared the Zel'dovich calculation to higher-order Lagrangian schemes and

shown that the perturbation theory appears to be converging quickly (see also Tassev 2014a). All of the Lagrangian perturbation theories provide a good match to the N-body results on scales above $20\,h^{-1}$Mpc.

The calculation has been extended to include biased tracers of the density field, including terms which are third order in the linear theory power spectrum. We have also considered non-local bias terms such as a dependence on tidal shear in the initial field. We find that these higher order terms are generally very small. The Zel'dovich approximation provides a very good fit to the real-space correlation function of halos found in N-body simulations, and to the monopole of the redshift-space correlation function. However, it does not match the quadrupole moment below $75\,h^{-1}$Mpc. Modifications to the bias terms which introduce a scale-dependence can improve the agreement with the N-body results, but usually at the expense of worsening the agreement in the monopole. We have argued that at least some of this disagreement is an issue with the approximation itself, and that it predicts the wrong pairwise velocity distribution for biased tracers.

Finally we have used the Zel'dovich approximation to compute the ingredients of the Gaussian streaming model of Reid & White (2011). We find that this hybrid model, which we refer to as the Zel'dovich streaming model and which involves only simple integrals of the linear theory power spectrum, provides a good match to the N-body measurements down to tens of Mpc.

REFERENCES

Baldauf T., Seljak U., Desjacques V., McDonald P., 2012, preprint [arXiv:1201.4827]
Bernardeau, F., Colombi, S., Gaztañaga, E., Scoccimarro, R., 2002, Physics Reports, 367, 1
Bond J.R., Couchman H.M.P., 1988, in the Proceedings of the Second Canadian Conference on General Relativity and Relativistic Astrophysics, p. 385
Buchert T., 1989, A&A, 223, 9
Carlson, J., Reid, B.A., White, M, 2013, MNRAS, 429, 1674
Chan K.C., Scoccimarro R., Sheth R., 2012, PRD, 85, 083509
Coles P., Lucchin F., 1995, "Cosmology: the origin and evolution of cosmic structure", John Wiley & Sons (London, 1995)
Coles P., Melott A.L., Shandarin S.F., 1993, MNRAS, 260, 765
Coles P., Sahni V., 1996, The Observatory, v.116, p.25-31
Doroshkevich A.G., Kotok E.V., Poliudov A.N., Shandarin S.F., Sigov Iu.S., Novikov I.D., 1980, MNRAS, 192, 321
Eisenstein D.J., Seo H.J., Sirko E., Spergel D.N., 2007, ApJ, 664, 675
Fisher K.B., 1995, ApJ, 448, 494
Fisher K.B., Nusser A., 1996, MNRAS, 279, 1
Gorski K., 1988, ApJ, 332, L7
Gurbatov S.N., Saichev A.I., Shandarin S.F., 2012, Physics Uspekhi, 55, 223
Hidding J., Shandarin S.F., van de Weygaert R., 2014, MNRAS, in press [arXiv:1311.7134]
Hivon E., Bouchet F.R., Colombi S., Juszkiewicz R., 1995, A&A, 298, 643
Matsubara T., 2008, Phys Rev D77, 063530
Matsubara T., 2008, Phys Rev D78, 083519
Matsubara, T., 2011, Phys Rev D83, 083518
McCullagh N., Szalay A., 2012, ApJ, 752, 21
McDonald P., Roy A., 2009, JCAP, 0908, 020
Melott A.L., Pellman T.F., Shandarin S.F., 1994, MNRAS, 269, 626
Moutarde F., Alimi J.-M., Bouchet F.R., Pellat R., Ramani A., 1991, ApJ, 382, 377
Munshi D., Sahni V., Starobinsky A.A., 1994, ApJ, 436, 517
Noh Y., White M., Padmanabhan N., 2009, Phys. Rev. D80, 123501
Okamura T., Taruya A., Matsubara T., 2011, JCAP, 8, 12
Pauls J.L., Melott A.L., 1995, MNRAS, 274, 99
Padmanabhan N., White M., Phys. Rev. D80, 063508
Padmanabhan N., White M., Cohn J.D., 2009, Phys. Rev. D79, 063523
Peacock J.A., 1999, "Cosmological physics", Cambridge University Press (Cambridge, 1999)
Peebles P.J.E., 1980, "The large-scale structure of the Universe", Princeton University Press (Princeton, 1980).
Porto R.A., Senatore L., Zaldarriaga M., 2014, preprint [arXiv:1311.2168]
Press W.H., Schechter P., 1974, ApJ, 187, 425
Reid B.A., White M., 2011, MNRAS, 417, 1913
Reid B.A., et al., 2012, MNRAS, 426, 2719 [arXiv:1203.6641]
Roth N., Porciani C., 2011, MNRAS, 415, 829
Sahni V., Coles P., 1995, Phys. Rep., 262, 1
Samushia L., Pericval W., Raccanelli A., 2012, MNRAS, 420, 2102
Schulz A., White M., 2006, Astroparticle Physics 25, 172 [astro-ph/0510100]
Seto N., Yokoyama J., 1998, ApJ, 492, 421
Shandarin S.F., Zel'dovich Ya.-B., 1989, Reviews of Modern Physics, 61, 185
Sheth R., Chan K.C., Scoccimarro R., 2012, preprint [arXiv:1207.7117]
Sheth R., Tormen G., 1999, MNRAS, 308, 119
Szalay A.S., 1988, ApJ, 333, 21
Tassev S., Zaldarriaga M., 2012a, JCAP, 4, 013
Tassev S., Zaldarriaga M., 2012b, JCAP, , 10, 006
Tassev S., Zaldarriaga M., 2012c, JCAP, 12, 011 [arXiv:1203.5785]
Tassev S., 2014a, preprint [arXiv:1311.4884]
Tassev S., 2014b, preprint [arXiv:1311.6316]
Taylor A.N., Hamilton A.J.S., 1996, MNRAS, 282, 767
Wang X., Szalay A., 2012, PRD, 86, 043508
Wang L., Reid B.A., White M., 2013, MNRAS, 437, 588
White M., 2002, ApJS, 579, 16
White, M., Blanton, M., Bolton, A., et al. 2011, ApJ, 728, 126
Yoo J., Seljak U., 2014, preprint [arXiv:1308.1093]
Yoshisato A., Morikawa M., Gouda N., Mouri H., 2006, ApJ, 637, 555
Zel'dovich, Y., 1970, A&A, 5, 84

APPENDIX A: THE SHEAR TERMS

In order to compute the contributions from any s^2 terms to the correlation function(s) we need to evaluate several two-point functions. The simplest expectation value is $\langle s^2(\mathbf{q})\rangle = (2/3)\langle\delta^2\rangle$, inde-

pendent of position. The next simplest is

$$\left\langle s_{ij}(\mathbf{q}_1)\delta(\mathbf{q}_2)\right\rangle = \left(\frac{1}{3}\delta_{ij} - \hat{q}_i\hat{q}_j\right)\mathcal{J}_1(q) \tag{A1}$$

where $\mathbf{q} = \mathbf{q}_2 - \mathbf{q}_1$ and $\mathcal{J}_1$ is defined below. Then, for example, $\left\langle s_{ij}(\mathbf{q}_1)\delta(\mathbf{q}_2)\right\rangle\left\langle s_{ij}(\mathbf{q}_1)\delta(\mathbf{q}_2)\right\rangle = (2/3)\mathcal{J}_1^2(q)$. By similar logic

$$\left\langle s_{ij}(\mathbf{q}_1)\Psi_m(\mathbf{q}_2)\right\rangle = \delta_{ij}\hat{q}_m\mathcal{J}_2 + \left[\delta_{jm}\hat{q}_i + \delta_{im}\hat{q}_j\right]\mathcal{J}_3 + \hat{q}_i\hat{q}_j\hat{q}_m\mathcal{J}_4 \tag{A2}$$

with

$$\left\langle s_{ij}(\mathbf{q}_1)\Psi_m(\mathbf{q}_2)\right\rangle\left\langle s_{ij}(\mathbf{q}_1)\Psi_n(\mathbf{q}_2)\right\rangle = 2\mathcal{J}_3^2\delta_{mn} + \hat{q}_m\hat{q}_n \times$$
$$\left[2\mathcal{J}_2^2 + 2\mathcal{J}_3^2 + \mathcal{J}_4^2 + 3\mathcal{J}_2\mathcal{J}_3 + 2\mathcal{J}_2\mathcal{J}_4 + 4\mathcal{J}_3\mathcal{J}_4\right] \tag{A3}$$

and

$$\left\langle s_{ij}(\mathbf{q}_1)\delta(\mathbf{q}_2)\right\rangle\left\langle s_{ij}(\mathbf{q}_1)\Psi_m(\mathbf{q}_2)\right\rangle = -\frac{2}{3}\hat{q}_m\,\mathcal{J}_1\,[2\mathcal{J}_3 + \mathcal{J}_4] \quad . \tag{A4}$$

Also

$$\begin{aligned}\left\langle s_{ij}(\mathbf{q}_1)s_{mn}(\mathbf{q}_2)\right\rangle &= \delta_{ij}\delta_{mn}\mathcal{J}_5 + \left[\delta_{im}\delta_{jn} + \delta_{in}\delta_{jm}\right]\mathcal{J}_6\\ &+ \left[\delta_{ij}\hat{q}_m\hat{q}_n + \delta_{mn}\hat{q}_i\hat{q}_j\right]\mathcal{J}_7\\ &+ \left[\delta_{im}\hat{q}_j\hat{q}_n + \delta_{in}\hat{q}_j\hat{q}_m + \delta_{jm}\hat{q}_i\hat{q}_n + \delta_{jn}\hat{q}_i\hat{q}_m\right]\mathcal{J}_8\\ &+ \hat{q}_i\hat{q}_j\hat{q}_m\hat{q}_n\mathcal{J}_9 \end{aligned} \tag{A5}$$

and thus the contraction

$$\begin{aligned}\langle s_{ij}&(\mathbf{q}_1)s_{mn}(\mathbf{q}_2)\rangle\langle s_{ij}(\mathbf{q}_1)s_{mn}(\mathbf{q}_2)\rangle =\\ &9\mathcal{J}_5^2 + 24\mathcal{J}_6^2 + 8\mathcal{J}_7^2 + 24\mathcal{J}_8^2 + \mathcal{J}_9^2\\ +\;&12\mathcal{J}_5\mathcal{J}_6 + 12\mathcal{J}_5\mathcal{J}_7 + 8\mathcal{J}_5\mathcal{J}_8 + 2\mathcal{J}_5\mathcal{J}_9\\ +\;&8\mathcal{J}_6\mathcal{J}_7 + 32\mathcal{J}_6\mathcal{J}_8 + 4\mathcal{J}_6\mathcal{J}_9\\ +\;&16\mathcal{J}_7\mathcal{J}_8 + 2\mathcal{J}_7\mathcal{J}_9 + 8\mathcal{J}_8\mathcal{J}_9 \end{aligned} \tag{A6}$$

The terms $\mathcal{J}_i$ all have argument q and are simple integrals over the linear theory power spectrum,

$$\mathcal{J}_1(q) = \int \frac{k^2\,dk}{2\pi^2} P_L(k)\,j_2(kq) \tag{A7}$$

$$\mathcal{J}_2(q) = \int \frac{k\,dk}{2\pi^2} P_L(k)\left[\frac{2}{15}j_1(kq) - \frac{1}{5}j_3(kq)\right] \tag{A8}$$

$$\mathcal{J}_3(q) = \int \frac{k\,dk}{2\pi^2} P_L(k)\left[-\frac{1}{5}j_1(kq) - \frac{1}{5}j_3(kq)\right] \tag{A9}$$

$$\mathcal{J}_4(q) = \int \frac{k\,dk}{2\pi^2} P_L(k)\,j_3(kq) \tag{A10}$$

$$\mathcal{J}_5(q) = \int \frac{k^2\,dk}{2\pi^2} P_L(k)\frac{-14j_0 - 25j_2 + 24j_4}{315} \tag{A11}$$

$$\mathcal{J}_6(q) = \int \frac{k^2\,dk}{2\pi^2} P_L(k)\frac{7j_0 + 5j_2 - 2j_4}{105} \tag{A12}$$

$$\mathcal{J}_7(q) = \int \frac{k^2\,dk}{2\pi^2} P_L(k)\frac{3j_2 - 4j_4}{21} \tag{A13}$$

$$\mathcal{J}_8(q) = \int \frac{k^2\,dk}{2\pi^2} P_L(k)\frac{-2j_2 - 2j_4}{21} \tag{A14}$$

$$\mathcal{J}_9(q) = \int \frac{k^2\,dk}{2\pi^2} P_L(k)\frac{-j_2 + 20j_4}{21} \tag{A15}$$

where we have suppressed the kq argument of the spherical Bessel functions in the last few equations. Note that $\mathcal{J}_5$ and $\mathcal{J}_6$ have non-zero limits as $q \to 0$ but all of the other terms vanish in this limit. It is easy to show that $\mathcal{J}_5 \to -(2/45)\langle\delta^2\rangle$ and $\mathcal{J}_6 \to (1/15)\langle\delta^2\rangle$ so that

$$\frac{\left\langle s_{ij}(0)s_{mn}(0)\right\rangle}{\langle\delta^2\rangle} \to -\frac{2}{45}\delta_{ij}\delta_{mn} + \frac{1}{15}\left[\delta_{im}\delta_{jn} + \delta_{in}\delta_{jm}\right] \tag{A16}$$

as $q \to 0$ and therefore

$$\left\langle s_{ij}(0)s_{ij}(0)\right\rangle \to \frac{2}{3}\langle\delta^2\rangle \tag{A17}$$

which agrees with our earlier result.

Numerically the largest contributions on scales above $20\,h^{-1}$Mpc are from $\mathcal{J}_3$ and $\mathcal{J}_4$. The next largest (in absolute magnitude) are $\mathcal{J}_1$, $\mathcal{J}_2$ and $\mathcal{J}_9$ and then $\mathcal{J}_8$. All terms are very smoothly varying functions of q, like their counterparts $\sigma^2(q)$ and $U(q)$ shown in Fig. 1.

Erratum:

The coefficients given in the integrals $\mathcal{J}_5 - \mathcal{J}_9$ are incorrect. They should read

$$\mathcal{J}_5(q) = \int \frac{k^2\,dk}{2\pi^2} P_L(k)\frac{-14j_0 - 40j_2 + 9j_4}{315} \tag{A18}$$

$$\mathcal{J}_6(q) = \int \frac{k^2\,dk}{2\pi^2} P_L(k)\frac{7j_0 + 10j_2 + 3j_4}{105} \tag{A19}$$

$$\mathcal{J}_7(q) = \int \frac{k^2\,dk}{2\pi^2} P_L(k)\frac{4j_2 - 3j_4}{21} \tag{A20}$$

$$\mathcal{J}_8(q) = \int \frac{k^2\,dk}{2\pi^2} P_L(k)\frac{-3j_2 - 3j_4}{21} \tag{A21}$$

$$\mathcal{J}_9(q) = \int \frac{k^2\,dk}{2\pi^2} P_L(k)\,j_4 \tag{A22}$$

The conclusions are unchanged.